Wavelength Measurements of IUE High Dispersion Spectra

Introduction

Tests were run to determine how accurately the wavelengths of high dispersion interstellar lines could be measured using the extracted spectral files produced by the IUE Spectral Image Processing System (IUESIPS), and the analysis software currently available at the IUE Regional Data Analysis Facilities (RDAFs). These tests were performed partly in response to a recent IUE Three-Agency Report by Stickland (ref. 1) which presented radial velocity measurements of Zeta Cas spectra using the IUEDR data analysis software currently available in the UK. In particular, the study hoped to determine the magnitude of variations in the high dispersion wavelength assignments, and whether the accuracy of the wavelength assignments varied with previous changes in the IUESIPS software.

Method

Flux and wavelength arrays were extracted from the standard IUESIPS MEHI files and calibrated using the RDAF routine IUESPEC. IUESPEC extracts the gross and background flux arrays, rederives a net flux, corrects for the echelle grating response (i.e. the IUE ripple-correction), and applies the inverse sensitivity function in a manner similiar to IUESIPS. A correction for THDA-sensitivity is also applied to the flux arrays although this is generally a minor correction (ref. 2). No corrections were applied to the wavelength arrays although a heliocentric velocity correction was applied to the four earliest images using the RDAF routine RADCOR, since these image were originally processed before this correction was added to IUESIPS. Note that both IUESIPS and RADCOR use IUE orbital elements obtained in 1980 and may therefore introduce errors on the order of a few km/sec due to changes in the IUE orbit.

The line measurements were derived using the RDAF routine FEATURE which calculates a flux-weighted mean wavelength within a region specified by the user. The laboratory wavelengths of the measured interstellar lines were provided by Bruhweiler (ref. 3). Eight interstellar absorption lines were measured from 13 high dispersion spectra of the standard star HD 3360 (i.e., Zeta Cas). These lines, and all but two of the images were analyzed by Stickland (ref. 1). The images were obtained between 1978 and 1989, and were processed by IUESIPS between 1980 and 1990. Two of the 13 spectra were small aperture exposures. Three of the earliest images were reprocessed to determine whether the reprocessing had any effect on the measured line positions. The differences between the measured and laboratory wavelengths were converted to velocities. The mean velocity difference was determined and the standard deviations were derived for

each of the 13 images and for each of the interstellar lines.

In addition to measuring interstellar lines, the program FEATURE was used to measure the wavelengths of artificially-generated line profiles (i.e., a Gaussian plus random noise). A program was written to generate Gaussian profiles resembling the interstellar line profiles seen in IUE high dispersion spectra. A 100-element array of values between 1200 and 1205 was generated with a Gaussian centered at 1202.5. A Gaussian width of 0.1 was used, which corresponded to about 8-9 data points per line. Pseudo-random noise was then added (i.e. uniformly distributed numbers between 0.0 and 1.0) using the intrinsic IDL command RANDOMU. The pseudo-line profiles were measured with both the RDAF routine FEATURE, and a Gaussian-fitting routine similiar to the RDAF program GAUSSFITS with a linear background fit. The magnitude of the added noise was varied to determine its effect on the wavelength measurements.

Results

The results of the Zeta Cas measurements are shown in Table 1. Column 6 represents the difference between the measured and the laboratory wavelength, expressed in units of velocity. The heliocentric velocity correction is included. The mean wavelength differences, standard deviations, date of processing, and applied heliocentric velocity corrections, are summarized in Table 2.

The mean radial velocity for 8 lines measured on 13 images was about -4.4 km/sec, with a mean standard deviation per image of 4.1 km/sec. After the 3 early images were reprocessed, the mean velocity was -4.1 km/sec with a mean standard deviation per image of 3.9 km/sec. The mean standard deviation per element was about 6.1 km/sec (using the reprocessed data). The largest deviation from the mean for a single line measurement was 22 km/sec. A sample plot produced by FEATURE is shown in Figure 1, where "WLAB" represents the laboratory wavelength and "Whet" is the measured value.

It should be pointed out, that the RDAF software rederives the absolutely-calibrated net flux from the gross and background flux arrays rather than starting with the ripple-corrected net flux stored in the MEHI files. Tests using lines measured directly from the ripple-corrected net flux array however, generally showed wavelength differences of less than 2 km/sec when compared to the results from the RDAF routine IUESPEC.

A sample of the pseudo-line profiles (as displayed by FEATURE) is shown in Figure 2. Figure 3 shows the results of repeating measurements such as these for different signal-to-noise ratios. The plot shows the differences between the measured positions and the known Gaussian center position after being converted to velocity units (assuming the line was located at 1202.5 angstroms). The '+' symbols represent estimated center postions using the flux-weighted mean value

derived by FEATURE. The diamonds are positions determined from a fitted Gaussian profile when applying the user-estimated edge points input to FEATURE. The results show that the accuracy of the line measurement varies with the signal/noise ratio such that lines with a signal/noise ratio of 1 can produce errors on the order of 10 km/sec, while lines with a signal/noise ratio of 6 are generally accurate to about 2 km/sec. A rough estimate of 2 for the signal/noise ratio of the Zeta Cas lines would imply a measurement accuracy of about +/- 5 km/sec.

Conclusions

As shown in Table 2, no obvious correlations were found between the Zeta Cas radial velocity measurements and the date of processing. It was found however that reprocessing 3 early images resulted in slightly reducing the mean velocity and the mean standard deviations. The primary change in IUESIPS that could affect the wavelength assignments would presumably be the revisions made to the mean dispersion relations and the corresponding temperature and time corrections. Originally, images were processed using only mean dispersion relations. In May 1981, the mean relations were corrected with a constant term which compensated for temperature and time variations (ref. 4). The SWP high dispersion relations have now been revised six times with the latest implementation in 1987 (ref. 5). The revisions have been necessary primarily because the time variations are not linear, and systematic errors have been found to occur when the dispersion relations are not updated every few years. It is interesting to note that, as shown in reference 5, the SWP high dispersion spectral format has shifted approximately 3 pixels or about 23 km/sec along the dispersion since the the wavelength calibration monitoring program began in 1979.

Our mean radial velocity measurements for images obtained prior to 1984 agree to within a few km/sec with Stickland's. After 1984, Sticklands values increase with mean radial velocities per spectrum as high as -21 km/sec, whereas our results show little, if any, variation. Perhaps this apparent velocity shift could be explained if the IUEDR wavelengths were derived from outdated dispersion relations or time corrections. If a linear (or outdated 2nd-order) time correction was being used, it would create systematic wavelength errors that would increase with time similiar to the results presented by Stickland.

The mean radial velocity of -4 km/sec seems to be in fairly good agreement with published optical data results which found radial velocities of -6 km/sec (ref. 6). Deviations of 10 to 20 km/sec in the individual line measurements, however, imply a larger uncertainty in single measurements. These variations appear larger than one would expect from the effects of random noise or user measurement error. They are also somewhat larger than reported in previous studies based on analyzing the wavelength assignments of high dispersion Pt-Ne lamp

exposures (ref. 6 and 7). Possible sources for these errors have been described in section 6.5 of the IUE Image Processing Manual (ref. 4).

As expected, tests with measuring positions of pseudo-gaussian features with added random noise, show that the errors in estimating center positions vary with the signal-to-noise ratio. For the interstellar lines such as those from the Zeta Cas spectra which have apparent signal/noise ratios of about 2, it seems reasonable to assume that wavelength measurements could vary over a range of plus or minus 5 km/sec, due solely to the effects of noise.

Randall W. Thompson

Ruth E. Bradley

Terry J. Teays

May 10, 1990

References

1) D. J. Stickland,'Record of the International Ultraviolet Explorer Three-Agency Meeting', F-71, November 15, 1989.

2) G. Sonneborn,'Record of the International Ultraviolet Explorer Three-Agency Meeting', A-60, November, 1984.

3) F. Bruhweiler, 1990, private communication.

4) B. E. Turnrose, R. W. Thompson,'International Ultraviolet Explorer Image Processing Information Manual, Version 2.0', section 6, 1984.

5) R. W. Thompson,'IUE Data Reduction XXXV. Implementation of New Dispersion Constants', NASA IUE Newsletter, 35, 108, 1988

6) J. N. Heckathorn, 'Study of the Accuracy of Wavelengths', Minutes of the Meeting of the International Ultraviolet Explorer Users Committee, Appendix H, September 1983.

7) R. W. Thompson,'Monitoring of Spectral Format Shifts', Minutes of the Meeting of the International Ultraviolet Explorer Users Committee, Appendix I, September 1983.

8) Wilson, R. E., 1963, General Catalogue of Stellar Radial Velocities, (Washington:Carnegie Institution), p. 7.

Table 1. IUE Wavelength Assignments of Interstellar Lines of High Dispersion Zeta Cas Spectra Using the RDAF Routine FEATURE

Element	SWP Image #	Wavelengths Lab	Measured	Difference A	*corr km/s
Si II	2022	1193.31	1193.208	-0.102	-3.8
	2022rep		1193.302	-0.008	-2.0
	5261		1193.285	-0.025	1.2
	7807		1193.363	0.053	-9.0
	7807rep		1193.264	-0.046	-11.6
	13928		1193.303	-0.007	0.7
	16298		1193.246	-0.064	-16.1
	16298rep		1193.255	-0.055	-13.8
	16299		1193.287	-0.023	-5.8
	19316		1193.257	-0.053	-13.3
	22047		1193.269	-0.041	-10.3
	30118		1193.280	-0.030	-7.5
	32365		1193.259	-0.051	-12.8
	34272		1193.259	-0.051	-12.8
	34749		1193.267	-0.043	-10.8
	37716		1193.290	-0.020	-5.0
N II	2022	1199.55	1199.433	-0.117	-7.4
	2022rep		1199.524	-0.026	-6.5
	5261		1199.548	-0.002	7.0
	7807		1199.598	0.048	-10.3
	7807rep		1199.518	-0.032	-8.0
	13928		1199.553	0.003	3.2
	16298		1199.500	-0.050	-12.5
	16298rep		1199.502	-0.048	-12.0
	16299		1199.527	-0.023	-5.7
	19316		1199.553	0.003	0.7
	22047		1199.502	-0.048	-12.0
	30118		1199.528	-0.022	-5.5
	32365		1199.518	-0.032	-8.0
	34272		1199.522	-0.028	-7.0
	34749		1199.542	-0.008	-2.0
	37716		1199.554	0.004	1.0
N I	2022	1200.22	1200.090	-0.130	-10.7
	2022rep		1200.208	-0.012	-3.0
	5261		1200.214	-0.006	6.0
	7807		1200.268	0.048	-10.3
	7807rep		1200.197	-0.023	-5.7
	13928		1200.239	0.019	7.2
	16298		1200.172	-0.048	-12.0
	16298rep		1200.177	-0.043	-10.7

	16299		1200.187	-0.033	-8.2
	19316		1200.207	-0.013	-3.2
	22047		1200.196	-0.024	-6.0
	30118		1200.215	-0.005	-1.2
	32365		1200.203	-0.017	-4.2
	34272		1200.177	-0.043	-10.7
	34749		1200.202	-0.018	-4.5
	37716		1200.233	0.013	3.2
S II	2022	1259.52	1259.404	-0.116	-5.8
	2022rep		1259.504	-0.016	-3.8
	5261		1259.515	-0.005	6.3
	7807		1259.547	0.027	-15.9
	7807rep		1259.467	-0.053	-12.6
	13928		1259.512	-0.008	0.6
	16298		1259.476	-0.044	-10.5
	16298rep		1259.477	-0.043	-10.2
	16299		1259.481	-0.039	-9.3
	19316		1259.483	-0.037	-8.8
	22047		1259.479	-0.041	-9.8
	30118		1259.472	-0.048	-11.4
	32365		1259.490	-0.030	-7.1
	34272		1259.465	-0.055	-13.1
	34749		1259.480	-0.040	-9.5
	37716		1259.491	-0.029	-6.9
Si II	2022	1260.42	1260.311	-0.109	-4.1
	2022rep		1260.400	-0.020	-4.8
	5261		1260.392	-0.028	0.8
	7807		1260.472	0.052	-9.9
	7807rep		1260.378	-0.042	-9.9
	13928		1260.449	0.029	9.4
	16298		1260.381	-0.039	-9.3
	16298rep		1260.387	-0.033	-7.8
	16299		1260.402	-0.018	-4.3
	19316		1260.401	-0.019	-4.5
	22047		1260.382	-0.038	-9.0
	30118		1260.397	-0.023	-5.5
	32365		1260.397	-0.023	-5.5
	34272		1260.380	-0.040	-9.5
	34749		1260.404	-0.016	-3.8
	37716		1260.416	-0.004	-1.0
Si II	2022	1304.37	1304.277	-0.093	0.4
	2022rep		1304.360	-0.010	-2.3
	5261		1304.382	0.012	10.3
	7807		1304.447	0.077	-4.0
	7807rep		1304.331	-0.039	-9.0
	13928		1304.440	0.070	18.6
	16298		1304.320	-0.050	-11.5
	16298rep		1304.324	-0.046	-10.6
	16299		1304.360	-0.010	-2.3
	19316		1394.376	0.006	1.4
	22047		1304.351	-0.019	-4.4
	30118		1304.369	-0.001	-0.2
	32365		1304.366	-0.004	-0.9
	34272		1304.353	-0.017	-3.9

	34749		1304.364	-0.006	-1.4
	37716		1304.395	0.025	5.7
Fe II	2022	1608.46	1608.292	-0.168	-9.5
	2022rep		1608.418	-0.042	-7.8
	5261		1608.444	-0.016	4.5
	7807		1608.489	0.029	-16.9
	7807rep		1608.387	0.073	-13.6
	13928		1608.496	0.036	10.8
	16298		1608.394	-0.066	-12.3
	16298rep		1608.402	-0.058	-10.8
	16299		1608.432	-0.028	-5.2
	19316		1608.432	-0.028	-5.2
	22047		1608.416	-0.044	-8.2
	30118		1608.418	-0.042	-7.8
	32365		1608.410	-0.050	-9.3
	34272		1608.414	-0.046	-8.6
	34749		1608.401	-0.059	-11.0
	37716		1608.462	0.002	0.4
C I	2022	1656.93	1656.752	-0.178	-10.4
	2022rep		1656.870	-0.060	-10.9
	5261		1656.941	0.011	9.5
	7807		1656.972	0.042	-14.7
	7807rep		1656.874	-0.056	-10.1
	13928		1656.985	0.055	12.4
	16298		1656.918	-0.012	-2.2
	16298rep		1656.929	-0.001	-0.2
	16299		1656.932	0.002	0.4
	19316		1656.945	0.015	2.7
	22047		1656.917	-0.013	-2.4
	30118		1656.910	-0.020	-3.6
	32365		1656.923	-0.007	-1.3
	34272		1656.907	-0.023	-4.2
	34749		1656.918	-0.012	-2.2
	37716		1656.942	0.012	2.2

*Note:
IUESIPS did not apply a heliocentric velocity correction until the fall of 1981. The four images above that were processed before this time were corrected using the RDAF routine RADCOR.
The images designated 'rep' were reprocessed with the current IUESIPS software.

Table 2. Zeta Cas Mean Wavelength Differences per Image and Element

Mean Wavelength Difference (lab - measured) per image:
("rep" = reprocessed images)

SWP Image #	Difference (km/s) Mean	Sigma	Date of Processing	*Helio. Vel. Corr.	Comments
2022	-6.4	3.9	3/25/80	21.8	small ap.
2022rep	-5.1	3.1	4/19/90	21.7	" "
5261	5.7	3.5	7/31/80	7.5	small ap.
7807	-11.4	4.3	1/31/80	-22.3	
7807rep	-10.1	2.6	4/19/90	-22.6	
13928	7.9	6.2	5/09/81	2.5	
16298	-10.8	4.0	2/12/82	-20.2	
16298rep	-9.5	4.1	4/19/90	-20.2	
16299	-5.1	3.1	2/12/82	-22.3	
19316	-3.8	5.4	2/27/83	-18.6	
22047	-7.8	3.2	1/19/84	-21.1	
30118	-5.3	3.7	1/19/87	-22.3	
32365	-6.1	4.0	11/22/87	-9.6	
34272	-8.7	3.5	3/07/89	9.9	
34749	-5.7	4.1	11/16/88	-8.0	
37716	-0.1	4.2	12/04/89	-14.9	
	---	---			
average	-4.4	4.1			
" (rep)	-4.1	3.9			

Mean Wavelength Difference per Element (using reprocessed data only):

Element	Lab Wavelength (angstroms)	Difference (km/sec) Mean	Sigma
Si II	1193.31	-8.0	5.4
N II	1199.25	-4.2	5.8
N I	1200.22	-3.2	5.7
S II	1259.52	-7.4	5.5
Si II	1260.42	-4.3	5.2
Si II	1304.37	0.1	7.8
Fe II	1608.46	-5.5	6.9
C I	1656.93	-0.6	6.6
		---	---
mean		-4.1	6.1

SWP 32365

WLAB	1259.520
W1	1259.365
W2	1259.502
W3	1259.604
RV1	−36.842
RV2	−4.300
RV3	20.106
F1	4.903E−09
F2	4.903E−09
F3	4.903E−09
F(cont)	4.903E−09
RESID(2)	1.000
EqW(mA)	135.414
Ftot	5.092E−10
Wtot	1259.478
WIDtot	0.083
Fnet	−6.640E−10
Wnet	1259.490
WIDnet	0.057

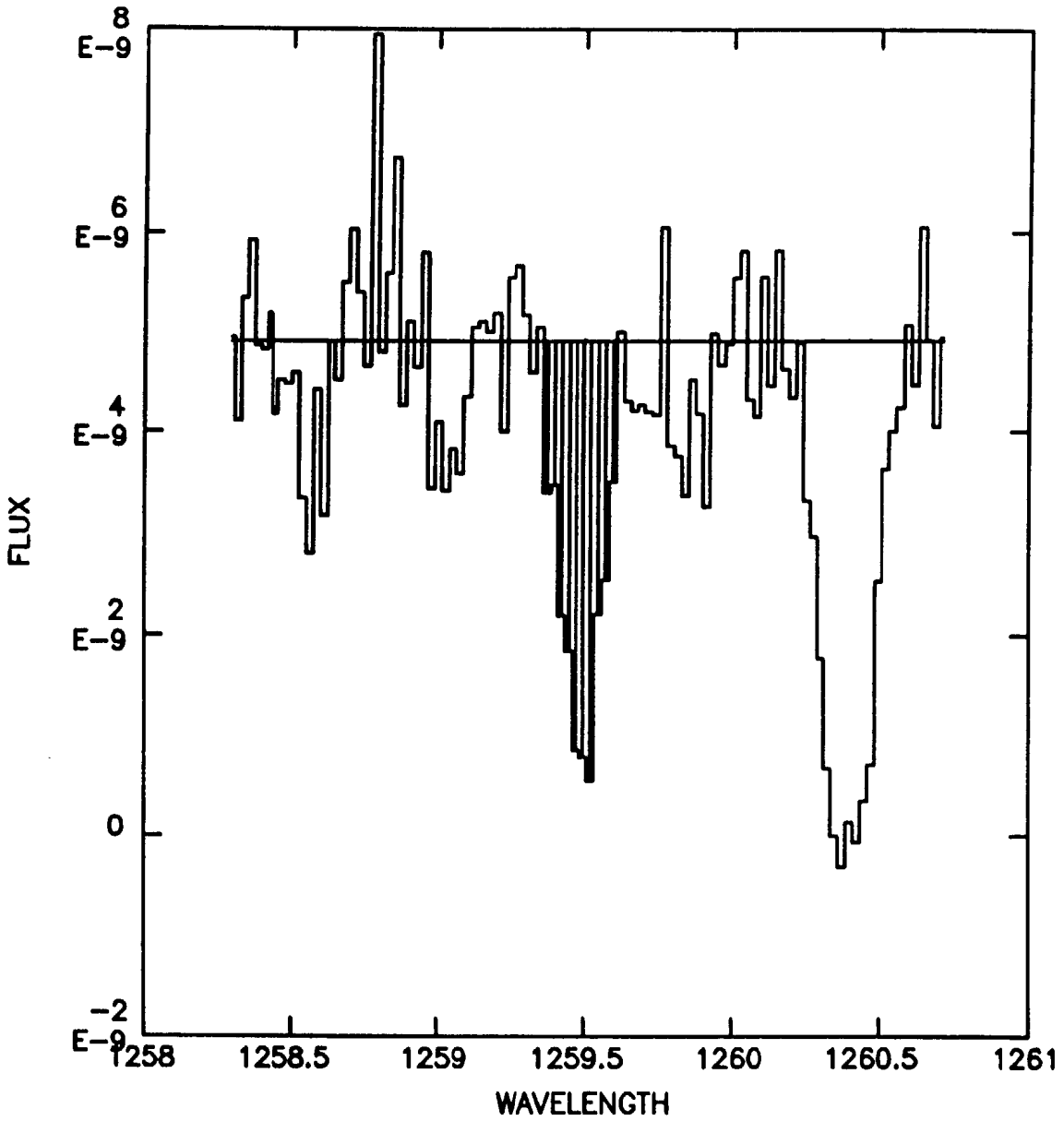

Figure 1. - Sample plot produced by FEATURE

WLAB	1202.500
W1	1202.284
W2	1202.511
W3	1202.764
RV1	−53.958
RV2	2.830
RV3	65.735
F1	3.278E−01
F2	−8.331E−01
F3	3.349E−01
F(cont)	3.314E−01
RESID(2)	−2.514
EqW(mA)	760.540
Ftot	−9.305E−02
Wtot	1202.554
WIDtot	0.109
Fnet	−2.521E−01
Wnet	1202.535
WIDnet	0.090

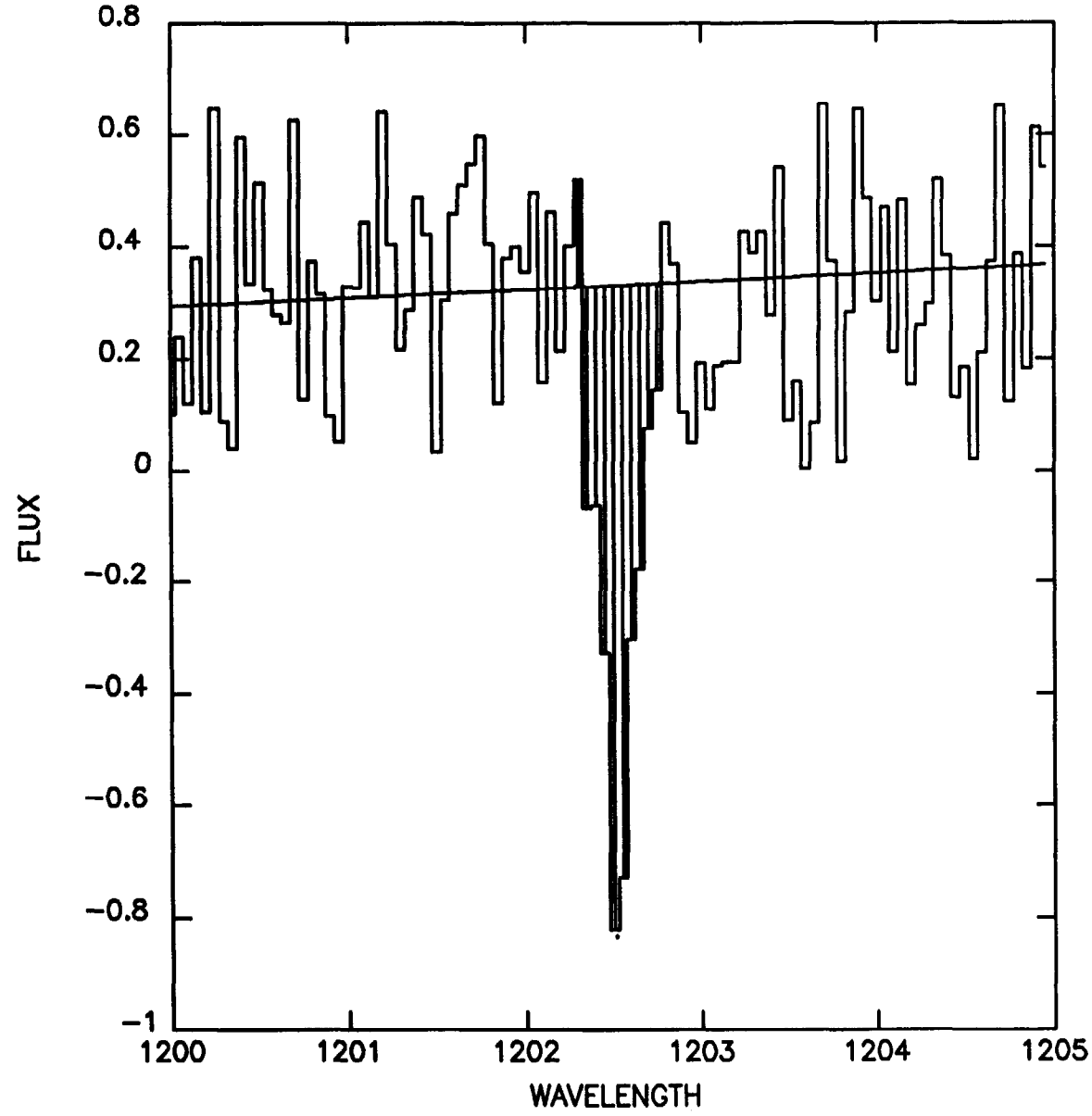

Figure 2. - Sample pseudo-line profile (S/N = 1:5)

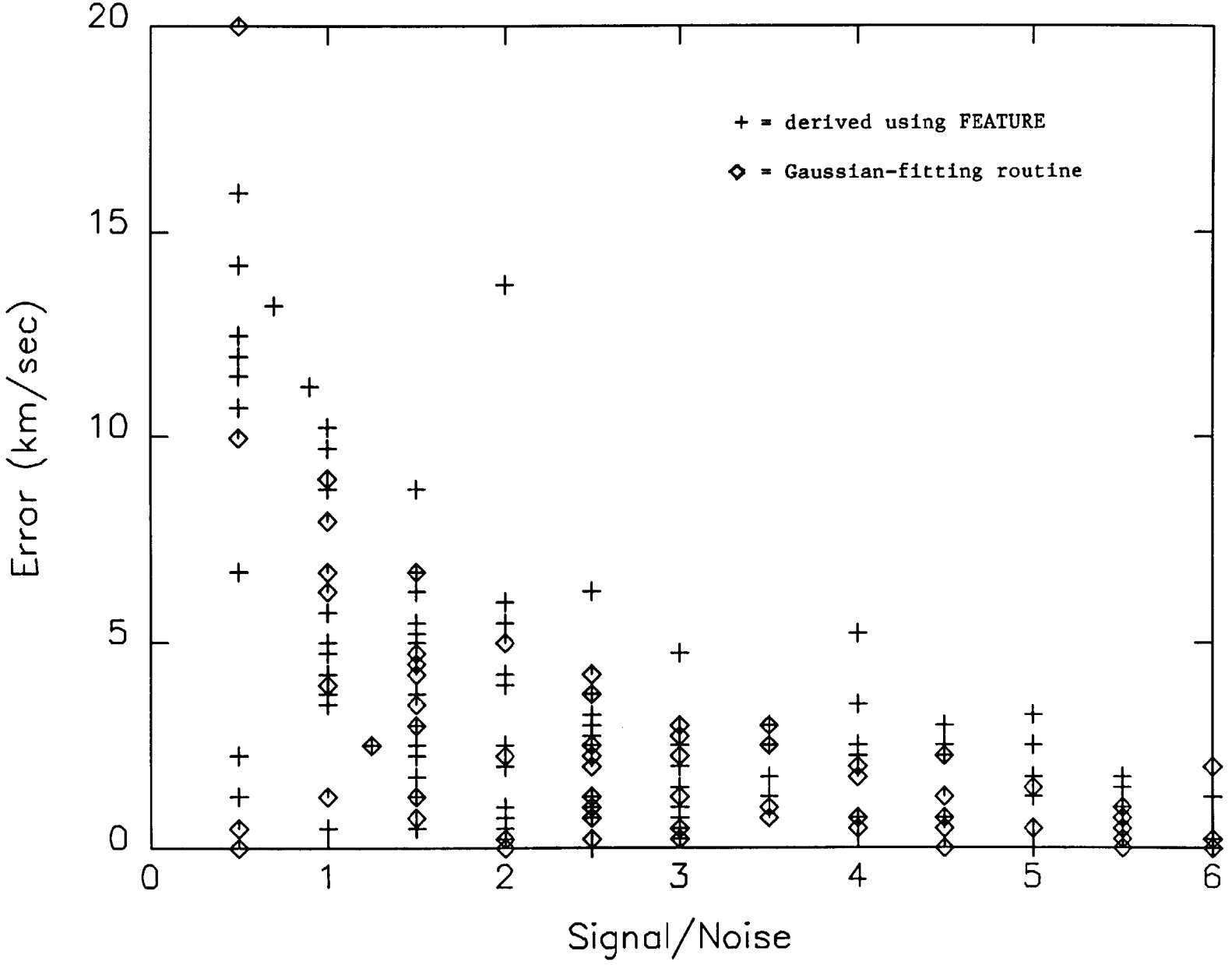

Figure 3 - Wavelength error as a function of S/N